International Journal of Power Electronics and Drive Systems (IJPEDS)
Vol. 15, No. 4, December 2024, pp. 2089~2096
ISSN: 2088-8694, DOI: 10.11591/ijpeds.v15.i4.pp2089-2096

Nonlinear robust control applied to the six-phase induction machine

Yarba Ahmed[1], Aichetoune Oumar[1], Mohamed Cherkaoui[2]
[1]Department of Physic, Faculty of Sciences and Technology, University of Nouakchott, Nouakchott, Mauritania
[2]Department of Electrical Engineering of Mohammedia School of Engineering (EMI), University Mohammed V in Rabat, Rabat, Morocco

Article Info

Article history:

Received Jul 17, 2023
Revised Apr 30, 2024
Accepted May 22, 2024

Keywords:

ADRC
Field-oriented control
Nonlinear robust control
SPIM
STSM

ABSTRACT

This paper proposes a nonlinear robust control for the six-phase induction machine (SPIM). It is based on the super twisting sliding mode (STSM) to ensure good decoupling and robust performance. This paper proposes also a comparative study between STSM and active disturbance rejection control (ADRC). We apply the rotor field-oriented control to ensure the decoupling between the magnitudes of the SPIM. Then we study the STSM control to regulate the rotor speed, the stator currents, and the rotor flux of the machine. The STSM ensures the same performance as the classical sliding mode control with the advantage of reducing the phenomenon of chattering. At the same time, the STSM command is compared to the ADRC command. The ADRC is one of the robust commands that makes it possible to estimate and eliminate internal or external disturbances. To test the robustness of the STSM and the ADRC, we implanted them in Simulink/MATLAB and the simulation results show the effectiveness of the STSM control compared to the ADRC control.

Corresponding Author:

Aichetoune Oumar
Department of Physic, Faculty of Sciences and Technology, University of Nouakchott
Nouakchott, Mauritania
Email: aichetouna.mahmoud@gmail.com

1. INTRODUCTION

In the field of high power which requires great reliability, the six-phase induction machine (SPIM) plays a very important role. The SPIM is a very popular multi-phase machine. It has multiple advantages compared with three-phase induction machines, such as segmentation, reliability, and minimization of rotor losses [1]-[4]. Many techniques of control are applied to the SPIM to control their magnitudes and to simplify its complexity, such as field-oriented control. however, the use of linear regulators makes the control sensitive to the variations of the internal and external parameters of the machine which is why modern techniques are used to increase the robustness of vector control such as sliding mode, active disturbance rejection control (ADRC), and fuzzy logic [5].

The sliding mode is a non-linear control, robust against parametric variations of the machine and disturbances. This approach has shown its performance in many research works [6]-[10]. Despite its advantages, the sliding mode still has disadvantages related to the phenomenon of chattering and other mechanical problems [7]. To eliminate these inconveniences, a method called super twisting sliding mode (STSM) is used which is an algorithm of the second-order sliding mode [11]. The STSM reduces the phenomenon of chattering [12]-[14]. The method aims to cancel the sliding surface and its drift in a finite time [15].

Another nonlinear controller is based on the approach of active disturbance rejection control. This control is inherited from the proportional-integral-derivative (PID) controller [16]. It is a robust control that estimates and compensates in real time the unknown dynamics and disturbances. The ADRC approach is established on the block called extended state observer (ESO) which is responsible for estimating internal and external disturbance [17]-[20].

Our aim in this work is to compare the STSM control and the ADRC control by applying these two approaches to control the SPIM. The purpose of the paper is to generate a robust controller based on the STSM technique which makes it possible to increase the robustness of the control against variations in machine parameters and load variation. It allows the stability of the machine to be maintained with greater speed, it also eliminates the chattering phenomenon which causes losses and wear to the mechanical system of the machine.

In this paper, the SPIM control applied is the rotor field-oriented control to ensure the decoupling between electromagnetic torque and the rotor flux. The rotor speed, stator current, and rotor flux were regulated by a STSM regulator the first time and by the ADRC regulator the second time, and a comparison between these two techniques. The paper is organized as i) We describe SPIM after we present the STSM and we will apply it to the control of SPIM; ii) We test the performance of the STSM control under load variation and we make a comparison between this control and the ADRC control, and iii) We finish with a conclusion.

2. PROPOSED METHOD

2.1. Super twisting sliding mode (STSM)

The classical sliding mode produces the phenomenon of chattering which generates a dangerous vibration of the system control. To reduce this vibration many solutions have been proposed, one of those solutions is the second-order sliding mode by applying the super twisting algorithm to ensure the convergence of the sliding surface and its derivative towards the origin in a finite time. The STSM controller is defined as the first higher-order sliding mode controller. This algorithm twists around the origin of the sliding plane and converges towards the origin of finite time with an infinite number of rotations [21]-[23].

Consider an input system u and x represent the state variable and y is the output defined by (1) and (2). The sliding mode error is defined by (3) and the STSM algorithm is defined by (4) and (5).

$$\frac{dx}{dt} = a(x,t) + b(x,t)u \tag{1}$$

$$y = c(x,t) \tag{2}$$

$$s = y^* - y \tag{3}$$

$$u = k_p s^r sgn(s) + u_1 \tag{4}$$

$$\frac{du_1}{dt} = k_i sgn(s) \tag{5}$$

The k_p, k_i, r are positive parameters. Where k_p, k_i represent the gains of the proportional and integral regulators. r is an exponent characterizing the STSM regulator. This approach retains the advantages of sliding mode and still eliminates the chattering phenomenon. Figure 1 illustrates the graphical representation of the STSM control.

2.2. Description of SPIM

The SPIM has two main parts: the stator and the rotor. the stator contains two three-phase windings, coupled in a star. The two windings are shifted by an angle α= 30°. The rotor of the machine is a squirrel cage [24], [25]. The voltage equations in the park reference are presented here by system 1, as in (6).

$$\begin{cases} V_{ds1} = R_{s1} i_{ds1} + \frac{d}{dt}\psi_{ds1} - \omega_s \psi_{qs1} \\ V_{ds2} = R_{s2} i_{xs2} + \frac{d}{dt}\psi_{ds2} - \omega_s \psi_{qs2} \\ V_{qs1} = R_{s1} i_{qs1} + \frac{d}{dt}\psi_{qs1} + \omega_s \psi_{ds1} \\ V_{qs2} = R_{s2} i_{qs2} + \frac{d}{dt}\psi_{qs2} + \omega_s \psi_{ds2} \\ 0 = R_r i_{dr} + \frac{d}{dt}\psi_{dr} - \omega_{gl} \psi_{qr} \\ 0 = R_r i_{qr} + \frac{d}{dt}\psi_{qr} + \omega_{gl} \psi_{dr} \end{cases} \tag{6}$$

With $\omega_{gl} = \omega_s - \omega_r$. The flux is defined as (7).

$$\begin{cases} \psi_{ds1} = L_{s1} i_{ds1} + L_m (i_{ds1} + i_{ds2} + i_{dr}) \\ \psi_{ds2} = L_{s2} i_{ds2} + L_m (i_{ds1} + i_{ds2} + i_{dr}) \\ \psi_{qs1} = L_{s1} i_{qs1} + L_m (i_{qs1} + i_{qs2} + i_{qr}) \\ \psi_{qs2} = L_{s1} i_{qs2} + L_m (i_{qs1} + i_{qs2} + i_{qr}) \\ \psi_{dr} = L_r i_{dr} + L_m (i_{ds1} + i_{ds2} + i_{dr}) \\ \psi_{qr} = L_r i_{qr} + L_m (i_{qs1} + i_{qs2} + i_{qr}) \end{cases} \quad (7)$$

The electromagnetic torque and the mechanical equation are expressed by (8) and (9) respectively [14].

$$C_e = P \frac{L_m}{L_m + L_r} (\psi_{dr} (i_{qs1} + i_{qs2}) - \psi_{qr} (i_{ds1} + i_{ds2})) \quad (8)$$

$$\frac{d}{dt} \omega_r = C_{em} - C_r - K_f \omega_r \quad (9)$$

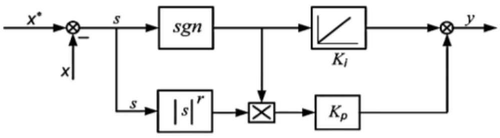

Figure 1. STSM control

2.3. STSM applied to SPIM

The application of the STSM command is represented in Figure 2. This figure shows us a set of elements such that one element represents the machine, another represents the converters, and others for controlling the machine in addition to an estimator of the angular speed and the rotor flux. All the speed, flux, and stator current regulation chains are controlled by the STSM controller.

2.3.1. STSM speed controller

To determine the STSM speed control law, we define the speed sliding mode surface given by (10).

$$s_\omega = \omega_r^* - \omega_r \quad (10)$$

Where ω_r^* is the speed reference and ω_r the measured speed. The STSM speed controller is used to determine the reference current i_{sq}^* (sum of direct stator currents i_{sq1}^* et i_{sq2}^*), given by (11).

$$i_{sq}^* = i_{sq1}^* + i_{sq2}^* \quad (11)$$

The output of the controller is defined by (12) and (13).

$$i_{sq}^* = k_{p\omega} s_\omega^r sgn(s_\omega) + i_{sq0}^* \quad (12)$$

$$\frac{di_{sq0}^*}{dt} = k_{i\omega} sgn(s_\omega) \quad (13)$$

2.3.2. STSM rotor flux controller

To define the STSM control law of the rotor flux, we define the rotor flux sliding mode surface as (14). Where φ_r^* represents the reference value of the rotor flux and φ_r is the estimated flux. The flux controller allows determining the reference current i_{sd}^* (sum of direct stator currents i_{sd1}^* et i_{sd2}^*), defined by (15).

$$s_\varphi = \varphi_r^* - \varphi_r \quad (14)$$

$$i_{sd}^* = i_{sd1}^* + i_{sd2}^* \quad (15)$$

The control law of the STSM controller of rotor flux is defined by (16) and (17).

$$i_{sd}^* = k_{p\varphi} s_\varphi^r sgn(s_\varphi) + i_{sd0}^* \quad (16)$$

$$\frac{di_{sd0}^*}{dt} = k_{i\varphi} sgn(s_\varphi) \quad (17)$$

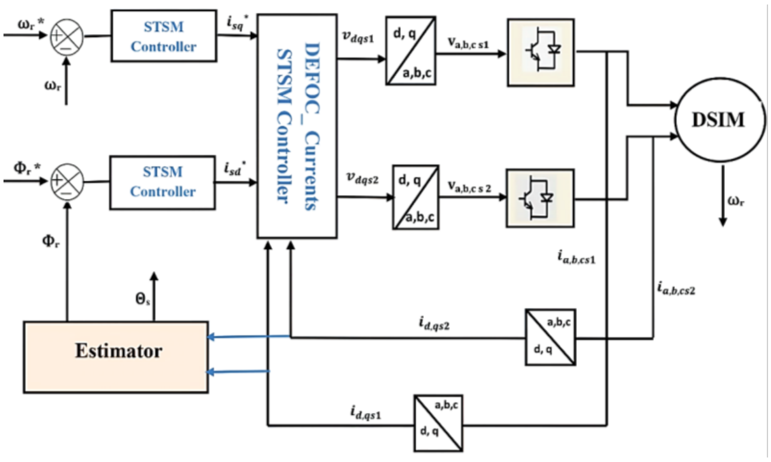

Figure 2. STSM control applied to the SPIM (DSIM)

2.3.3. STSM stator current controllers

In this part, we determine the STSM controller of the current component i_{sd1}, the other current controllers (i_{sd2} , i_{sq1}, i_{sq2}) are determined in the same way as i_{sd1}. The sliding surface of i_{sd1} is defined by (18). $i_{sd1}{}^{*}$ represents the current reference of i_{sd1}. The STSM current controller is used to calculate the reference voltage v_{sd1} defined by (19) and (20).

$$s_{d1} = i_{sd1}{}^{*} - i_{sd1} \tag{18}$$

$$v_{sd1} = k_{pd1} s_{d1}{}^{r} sgn(s_{d1}) + v_{sd10}{}^{*} \tag{19}$$

$$\frac{dv_{sd10}{}^{*}}{dt} = k_{id1} sgn(s_{d1}) \tag{20}$$

3. SIMULATION RESULTS

To verify the robustness and the performance of the proposed control based on the STSM control, we implement the configuration of Figure 2 in MATLAB/Simulink as shown in Figure 3. In this section, we studied two tests: in the first test, we simulated the STSM control applied to the DSIM under load variation while in the second test, we made a comparison between the STSM control with the ADRC control (the configuration presented in the reference [26], [27]). The coefficients for the STSM controllers are determined by the same method presented in the reference [22].

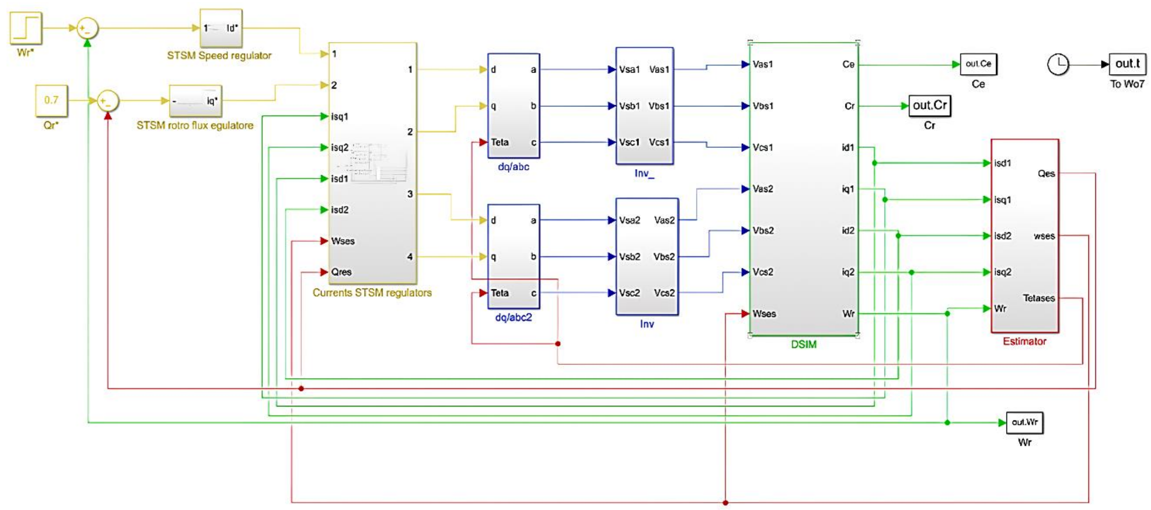

Figure 3. STSM control applies to the SPIM, Simulink block

3.1. Simulation of the STSM under load variation

The purpose of this test is to simulate the STSM control under load variation. The simulation conditions are as follows: i) The machine runs empty. In 2s we change the load torque from 0 to 10 N.m; ii) The reference speed is fixed at 100 rad/s; and iii) The rotor flux is maintained constant at 0.7 Wb. The results of the simulation of the load test are shown in Figures 4-7. Figures 4-7 present the variation of the rotor speed, the electromagnetic torque, the rotor flux, and the stator current respectively. From Figure 4, we can see that the speed tracks its reference value with a neglected surpass. The torque in turn presented in Figure 5 follows its setpoint with a starting torque of 18 N.m. The rotor flux illustrated by Figure 6 is maintained at 0.7 Wb and independent of the variation of the torque. At the level of the stator current isa1, as shown in Figure 7, it is clear that the curve is perfectly sinusoidal. We conclude from this test that the STSM proves its effectiveness in the load variation and maintains the rotor flux independent to the electromagnetic torque.

3.2. Comparison between STSM and ADRC controls

This section aims to verify the robustness and the performance of STSM by comparing it with the ADRC control cited in the reference [26], [27]. Both configurations are simulated under the same simulation conditions in section 3.1. Two tests are presented in this part. The first represents the load variation test and the second is the robustness test.

3.2.1. Load variation

The comparison is made between the STSM control and the ADRC control under the load variation. Figures 8-10 represent the simulation results of two configurations cited (ADRC-STSM). Figure 8 shows the rotor speed variation of the STSM and the ADRC. We can note that the STSM has a faster response than the ADRC. The STSM speed has a neglecting overtaking at the beginning but the ADRC doesn't' have it.

From Figure 9, we can see that the electromagnetic torque of the two configurations tracks its reference. We remark that the starting torque of the ADRC is 18.5 N.m and 17 N.m for the STSM. The response from the STSM is faster than the ADRC. About the current isa1, we note that the two curves of the STSM and the ADRC are sinusoidal. We conclude from this test that the STSM has a faster dynamics response than the ADRC and reduces the starting torque.

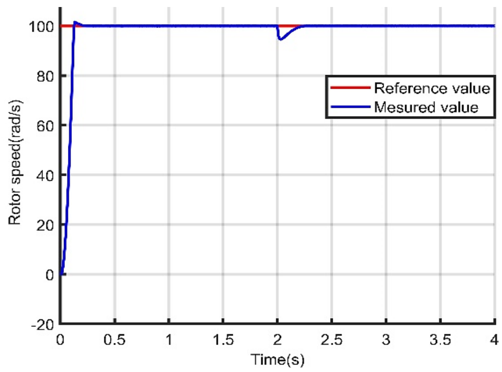

Figure 4. Speed of STSM control under load variation

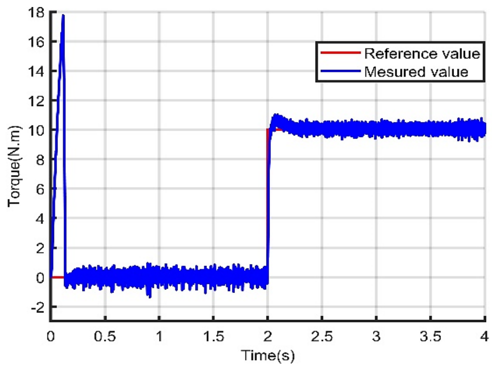

Figure 5. Torque of STSM control under load variation

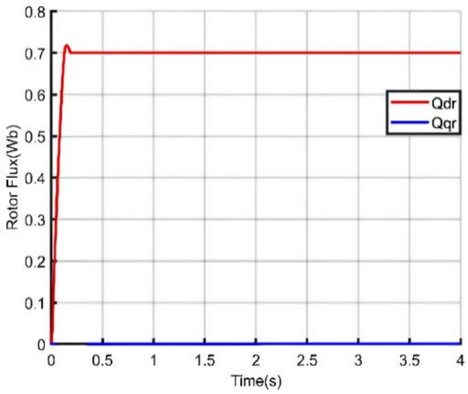

Figure 6. Rotor flux of STSM control under load variation

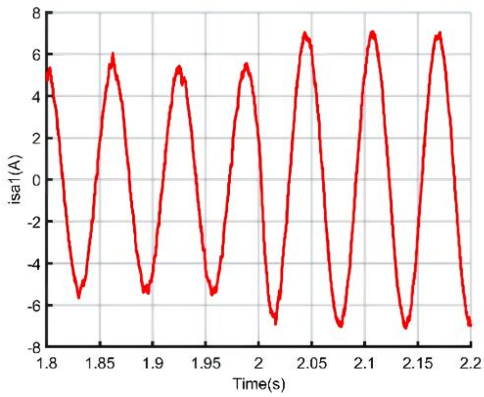

Figure 7. Stator current (isa1) of STSM control under load variation

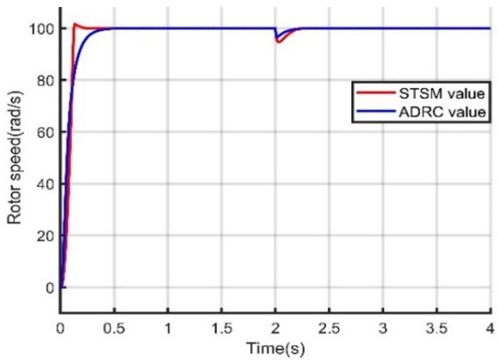

Figure 8. Speed of ADRC STSM under load variation

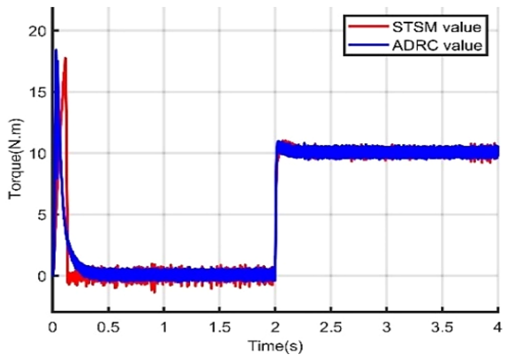

Figure 9. ADRC & STSM torque under load variation

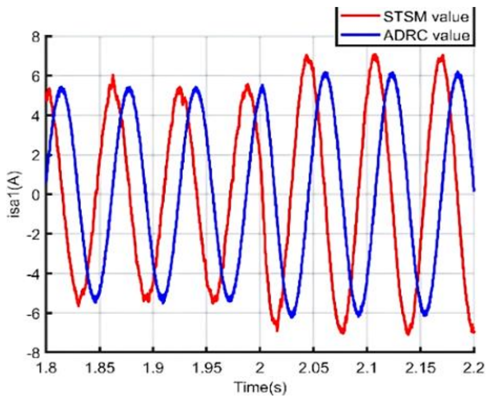

Figure 10. Current isa1 of STSM &ADRC under load variation

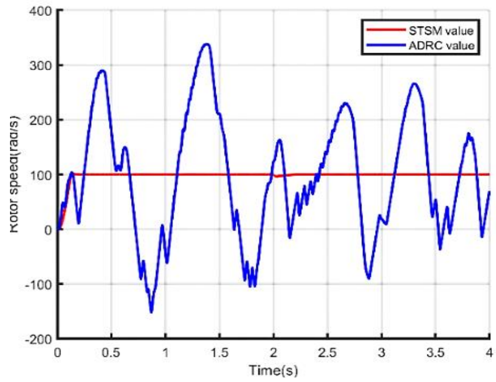

Figure 11. Speed of STSM &ADRC under a variation of 50% Rr & 30% j

3.2.2. Robustness test

The robustness test consists of varying the rotor resistance and the moment of inertia of the machine at the same time. Figures 11-13 illustrate the evolution of the rotor speed, electromagnetic torque, and the stator current during the variation of the rotor resistance to 50% of its nominal value and at the same time varying the moment of inertia by 30% of its nominal value. From Figures 11 and 12 we can see that the rotor speed and torque of STSM follow their reference values, unlike the ADRC speed and torque where is clear that these curves have strong ripples and oscillations. The stator current in turn as shown in Figure 13 is always sinusoidal. The ADRC current isn't sinusoidal and has a strong oscillation. In conclusion, these results show the fragility of the ADRC control against variations in rotor resistance and inertia at the same time. It also shows us the robustness of the STSM.

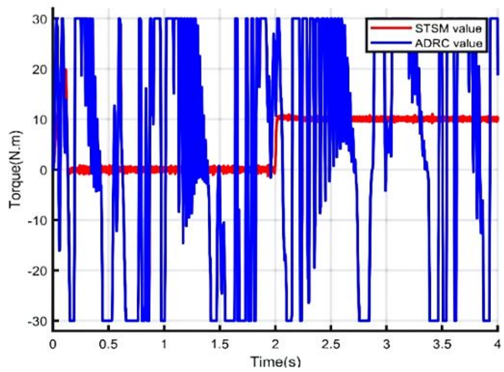

Figure 12. Torque of STSM &ADRC under a variation of 50% of Rr & 30% of j

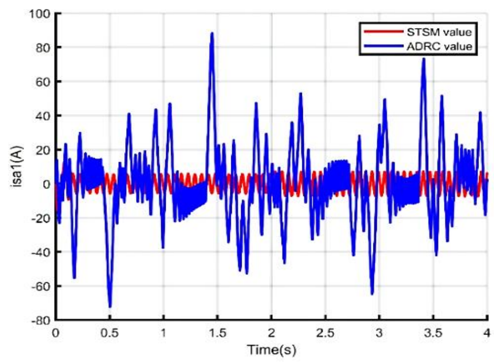

Figure 13. Current isa1 of the STSM &ADRC under a variation of 50% of Rr & 30% of j

4. CONCLUSION

The paper above presents a comparison study between two major controls which are the STSM and the ADRC. Each command is implemented and simulated in Simulink/MATLAB. The effectiveness of the STSM has been tested and has been compared with ADRC control under different operating conditions (load variation, variations of the rotor resistance, and the moment of inertia). The two controls have shown their robustness and performance against load variations and have also ensured the decoupling between the magnitudes of the SPIM. The STSM control has shown that is fast with more precision compared to the ADRC, it also proves robustness against the variations of the rotor resistance and the moment of inertia. The ADRC control in turn has shown that is very sensitive to the variation of machine parameters and has a slower response time than the STSM. The main contributions of this work are i) The application of STSM to control the SPIM allows to take into account the variation of two parameters of the machine at the same time; ii) The ripples of the torque and the rotor flux are reduced; and iii) A comparison between STSM and ADRC is made. In future studies, we want to test the robustness of STSM control in case of failure of SPIM sensors.

REFERENCES

[1] P. S. Dainez, E. Bim, D. Glose, and R. M. Kennel, "Modeling and parameter identification of a double-star induction machines," in *2015 IEEE International Electric Machines & Drives Conference (IEMDC)*, IEEE, May 2015, pp. 749–755. doi: 10.1109/IEMDC.2015.7409143.

[2] R. Sadouni and A. Meroufel, "Indirect rotor field-oriented control (IRFOC) of a dual star induction machine (DSIM) using a fuzzy controller," *Acta Polytechnica Hungarica*, vol. 9, no. 4, pp. 177–192, 2012.

[3] F. Naceri, T. Laamayad, S. Belkacem, and M. Benbrahim, "Fuzzy sliding mode speed controller design of induction motor drives," in *Proceedings of the 2012 International Conference on Industrial Engineering and Operations Management Istanbul, Turkey, July 3 – 6, 2012*, 2012, pp. 1330–1339.

[4] E. J. Akpama and L. U. Anih, "Modelling and simulation of multiphase induction machine," *International Journal of Engineering Innovation & Research*, vol. 4, no. 5, pp. 732–736, 2015, [Online]. Available: https://www.ijeir.org/administrator/components/com_jresearch/files/publications/IJEIR_1704_Final.pdf

[5] M. Ben Slimene and M. A. Khlifi, "Modeling and digital field-oriented control for double star induction motor drive," *International Journal of Applied Electromagnetics and Mechanics*, vol. 56, no. 4, pp. 511–520, Mar. 2018, doi: 10.3233/JAE-160136.

[6] B. B. Sereir, A. Tahour, and A. Aissaoui, "Speed sensorless control of an asynchronous asynchronous machine (La commande sans capteur de vitesse d'une machine asynchrone double étoile)," *Revue Roumaine des Sciences Techniques Électrotechnique et Énergétique*, vol. 63, no. 314–319, 2018, [Online]. Available: http://revue.elth.pub.ro/upload/11795113_ATahour_RRST_3_2018_pp_314-319.pdf

[7] N. Layadi, S. Zeghlache, F. Berrabah, and L. Bentouhami, "Comparative study between sliding mode control and backstepping control for double star induction machine (DSIM) under current sensor faults," *International Journal of Information Technology and Electrical Engineering*, vol. 6, no. 6, pp. 67–77, 2017.

[8] A. Massoum, A. Meroufel, and A. Bentaallah, "Sliding mode speed controller for a vector controlled double star induction motor," *Electrical Review Przegląd Elektrotechniczny*, 2012.

[9] O. Moussa, R. Abdessemed, S. Benaggoune, and et H. Benguesmia, "Sliding mode control of a grid-connected brushless doubly fed induction generator," *European Journal of Electrical Engineering*, vol. 21, no. 5, pp. 421–430, 2019.

[10] H. Amimeur, D. Aouzellag, R. Abdessemed, and K. Ghedamsi, "Sliding mode control of a dual-stator induction generator for wind energy conversion systems," *International Journal of Electrical Power & Energy Systems*, vol. 42, no. 1, pp. 60–70, Nov. 2012, doi: 10.1016/j.ijepes.2012.03.024.

[11] A. Q. Al-Dujaili, A. Falah, A. J. Humaidi, D. A. Pereira, and I. K. Ibraheem, "Optimal super-twisting sliding mode control design of robot manipulator: Design and comparison study," *International Journal of Advanced Robotic Systems*, vol. 17, no. 6, p. 172988142098152, Nov. 2020, doi: 10.1177/1729881420981524.

[12] O. Moussa, R. Abdessemed, and S. Benaggoune, "Super-twisting sliding mode control for brushless doubly fed induction generator based on WECS," *International Journal of System Assurance Engineering and Management*, vol. 10, no. 5, pp. 1145–1157, Oct. 2019, doi: 10.1007/s13198-019-00844-3.

[13] Z. Dekali, L. Baghli, and A. Boumediene, "Improved super twisting based high order direct power sliding mode control of a connected DFIG variable speed wind turbine," *Periodica Polytechnica Electrical Engineering and Computer Science*, vol. 65, no. 4, pp. 352–372, Oct. 2021, doi: 10.3311/PPee.17989.

[14] I. Sami, S. Ullah, A. Basit, N. Ullah, and J. Ro, "Integral super twisting sliding mode based sensorless predictive torque control of induction motor," *IEEE Access*, vol. 8, pp. 186740–186755, 2020, doi: 10.1109/ACCESS.2020.3028845.

[15] M. Horch, A. Boumediene, and L. Baghli, "Backstepping approach for nonlinear super twisting sliding mode control of an induction motor," in *2015 3rd International Conference on Control, Engineering & Information Technology (CEIT)*, IEEE, May 2015, pp. 1–6. doi: 10.1109/CEIT.2015.7233109.

[16] J. Han, "From PID to active disturbance rejection control," *IEEE Transactions on Industrial Electronics*, vol. 56, no. 3, pp. 900–906, Mar. 2009, doi: 10.1109/TIE.2008.2011621.

[17] X. Hua, D. Huang, and S. Guo, "Extended state observer based on ADRC of linear system with incipient fault," *International Journal of Control, Automation and Systems*, vol. 18, no. 6, pp. 1425–1434, Jun. 2020, doi: 10.1007/s12555-019-0052-2.

[18] F. Alonge, M. Cirrincione, F. D'Ippolito, M. Pucci, and A. Sferlazza, "Active disturbance rejection control of linear induction motor," *IEEE Transactions on Industry Applications*, vol. 53, no. 5, pp. 4460–4471, 2017.

[19] Y. Zhang, P. Zhang, C. Ran, and X. Zhang, "An active disturbance rejection control design method based on disturbance separation," *Journal of Physics: Conference Series*, vol. 1848, no. 1, p. 012127, Apr. 2021, doi: 10.1088/1742-6596/1848/1/012127.

[20] G. Herbst, "A simulative study on active disturbance rejection control (ADRC) as a control tool for practitioners," *Electronics*, vol. 2, no. 3, pp. 246–279, Aug. 2013, doi: 10.3390/electronics2030246.

[21] A. Garg and S. Narayan, "Super-twisting algorithm based sliding mode control of buck converter," *International Journal of Advance Research and Innovative Ideas In Education IJARIIE*, vol. 5, no. 3, pp. 1913–11922, 2019, [Online]. Available: https://ijariie.com/AdminUploadPdf/Super_Twisting_Algorithm_based_Sliding_Mode_Control_of_Buck_Converter_ijariie10544.pdf

[22] C. Lascu, A. Argeseanu, and F. Blaabjerg, "Supertwisting sliding-mode direct torque and flux control of induction machine drives," *IEEE Transactions on Power Electronics*, vol. 35, no. 5, pp. 5057–5065, May 2020, doi: 10.1109/TPEL.2019.2944124.

[23] J. Listwan, "Application of super-twisting sliding mode controllers in direct field-oriented control system of six-phase induction motor: experimental studies," *Power Electronics and Drives*, vol. 3, no. 1, pp. 23–34, Dec. 2018, doi: 10.2478/pead-2018-0013.

[24] A. Oumar, R. Chakib, and M. Cherkaoui, "Performance and characteristics of double star induction machine," in *2019 8th International Conference on Systems and Control (ICSC)*, IEEE, Oct. 2019, pp. 399–404. doi: 10.1109/ICSC47195.2019.8950582.

[25] A. Oumar, R. Chakib, M. Labbadi, and M. Cherkaoui, "Robust nonlinear controller of the speed for double star induction machine in the presence of a sensor fault," *International Journal of Intelligent Engineering and Systems*, vol. 13, no. 3, pp. 124–133, Jun. 2020, doi: 10.22266/ijies2020.0630.12.

[26] A. Oumar, R. Chakib, and M. Cherkaoui, "Modeling and control of double star induction machine by active disturbance rejection control," *TELKOMNIKA (Telecommunication Computing Electronics and Control)*, vol. 18, no. 4, pp. 2718–2728, Oct. 2020, doi: 10.12928/telkomnika.v18i5.14377.

[27] A. Oumar, R. Chakib, and M. Cherkaoui, "Current sensor fault-tolerant control of DSIM controlled by ADRC," *Mathematical Problems in Engineering*, vol. 2020, pp. 1–10, Aug. 2020, doi: 10.1155/2020/6568297.

BIOGRAPHIES OF AUTHORS

Yarba Ahmed is a director of a Training Center, Safety, and Nuclear Security at the University of Nouakchott in Mauritania. He received his Ph.D. degree from the National Engineers School of Tunis, El Manar, Tunis, in 2002. He also received his master's degree from this school in 1996. He was a professor at the University of Tunis and the King Faisal University in Arabie Saoudite. In 2009, he moved to the Faculty of Sciences and Technology in Mauritania. He was the head of the Department of Physics at the Faculty of Science. He can be contacted at email: yarba.ahmed.taleb@gmail.com.

Aichetoune Oumar received a Ph.D. degree from Mohammadia School of Engineers, Mohammed V University in Rabat, 2021. She received an engineering degree in Electromechanical Engineering from the Polytechnic of Nouakchott, Mauritania in 2016. Her research focuses on induction machine control, power electronics, sensorless drives for AC machines, and renewable energy. She can be contacted at email: aichetouna.mahmoud@gmail.com.

Mohamed Cherkaoui is an expert with the Moroccan Ministry for Higher Education and with industrialists on matters related to energetic efficiency. He received the engineer degree in Electrical Engineering, from Mohammedia Engineering School (EMI), Rabat, Morocco, in 1979. He received his Ph.D. degree from Institut National Polytechnique de Lorraine, Nancy, France in 1985. In 1986, he joined the University of Caddi Ayyad of Marrakech as a research professor. In 1995, he moved to the Mohammedia Engineering School (EMI), Rabat, as a professor of higher education and head of the Electrical Engineering Department. He was a director of the research laboratory in electrical power and control of the Mohammedia Engineering School (EMI), Rabat, Morocco. He can be contacted at email: cherkaoui@emi.ac.ma.